Water usability: a descriptive parameter of thermodynamic properties and water mobility in glucose/whey protein isolates composite solid matrices

Fanghui Fan (fanghui.fan@szu.edu.cn)
Shenzhen University
Tingting Cui
Shenzhen Univeristy
Xukai Wu
Shenzhen University
Tian Mou
Shenzhen University

Article

Keywords: Water mobility, aw, microbial growth, solid foods, food preservation

Posted Date: February 2nd, 2023

DOI: https://doi.org/10.21203/rs.3.rs-2368854/v1

Version of Record: A version of this preprint was published at npj Science of Food on June 14th, 2023.
See the published version at https://doi.org/10.1038/s41538-023-00207-0.

Abstract

A classic problem in preservation is the microbes can grow in low-moisture foods. In this paper, the water sorption and thermodynamic properties of glucose/*WPI* solid matrices were measured, while their molecular mobility was analyzed and associated with the microbial growth of *D. Hansenii* at various a_w and 30 ºC. Although the sorption isotherms, T_g, and relaxation processes of studied matrices were affected by a_w and *WPI*, the microbial growth showed highly dependent on water mobility rather than a_w. Hence, we introduced water usability (U_w), derived from the mobility difference between system-involved water and liquid pure water explicating from the classical thermodynamic viewpoint, to describe the dynamic changes of water mobility in glucose/*WPI* matrices. Despite to a_w, the yeast growth rate was enhanced at high U_w matrices concomitantly with a rapid cell doubling time. Therefore, the proposed U_w provides a better understanding of the water relationships of microorganisms in food preservation.

Introduction

The microbial response is a primary consideration for the quality and processability evaluation in food preservation due to the public health implications[1,2]. For instance, microbial growth may lead to alteration of the physicochemical properties of foods, which in turn may affect the shelf-life or become life-threatening in a certain case[3,4]. In general, food is a complex and dynamically heterogeneous system consisting of a myriad of biomaterials and solvents, which can collectively determine the microbial response in final products, *i.e.*, the survival and growth demanded carbon and nitrogen sources are satisfied by sugars and proteins[5]. Water, as a major solvent in foods, can provide a hospitable environment to support microbial growth, whereas removing water by simultaneously transferring heat and mass effectively inhibits the growth of spoilage and pathogenic microorganisms in foods[6,7]. However, such dehydration process seems not a reliable method for food preservation as pathogenic microorganisms have been shown to survive for several days, weeks, and even months or years in low-moisture foods. For example, *Aspergillus flavus* has been detected in baked foods[8]; *Salmonella* and *Cronobacter sakazakii* can contaminate powdered milk[9]. As more cases related to low-moisture foods as a vehicle for the foodborne disease are recorded worldwide, the rationale of microbial growth in food solids becomes a great challenge and needs to be understood, comprehensively.

For half a century, water activity (a_w) has become a critical indicator responsible for governing spoilage and pathogenic microorganisms in foods, principally because the measured a_w values generally correlate well with the potential for the growth and metabolic activity of microbes[7]. However, the physicochemical properties of solids in low-moisture food are often time-dependent, and the use of a_w should always consider the possible influences of nonequilibrium situations, such as glassy or crystallizable components, and thus, the a_w alone may be inappropriate to describe the attributes of these systems[10,11]. Previous studies have reported a temperature range of glass transition (T_g) considered as a physicochemical boundary to control the physicochemical properties as well as microbial growth in low-

moisture foods as the viscosity of the system increases as T_g increases[12,13]. Unfortunately, reality does not always appear to follow this scheme. Some xerophytic microbes, *e.g.*, *Aspergillus flavus, Xeromyces bisporus*, *Chrysosporium fastidium* have been found in solid foods and spoilage may not be prevented by keeping the product below its T_g value with high viscous situations[8,14]. Although the a_w is a solvent property and T_g refers to a property related to the structure of the solute matrix, both of them are strongly dependent on water involved in solid systems. Therefore, knowledge of both a_w and T_g needs a better understanding of the water behavior in solid foods.

The increasing evidence proposed that complementing a_w with water mobility dynamics may be an attribute that deserves further attention as the water mobility in low-moisture foods was highly correlated to many necessary diffusion-limiting processes to the growth and metabolic activity of microorganisms. For example, the *NMR* relaxation studies indicated that the water mobility-derived relaxation times (τ) were linear with the lag phase of *Staphylococcus aureus* [15], and the translational mobility of water could provide alternative measures than a_w for predicting the germination of *Aspergillus niger*[16]. Such experimental facts indicate that water mobility is necessary for the transportation of nutrients and metabolites for the growth of microorganisms, and thus, a more dependable and precise quantification of water mobility in low-moisture food needs to carefully propose[13]. Numerous publications have independently used relaxation times as a measure of water mobility and the T_g as an indicator of the overall mobility of the food system[17,18]. However, few studies provide descriptive on relationships between water and solids mobility and the T_g in solid foods and their potential applications to effectively inhibit or retard microbial growth.

To take into account the rate of variation in molecular mobility while crossing T_g, our previous works have defined the classification for solid-food systems: *Strength* parameter, S[19,20]. The S concept, identifying an allowable temperature range increases above T_g, is a parameter descriptive of the physical state of all components (including water) involved in solid foods as it intuitively expresses the spatiotemporal responsibility of molecules to change in motion. Besides, the Deborah number was applied to provide an useful translation of measured τ to real experimental timescales in S parameter. It should note that the types and speeds of mobility of water are dependent on temperature and external pressure, and in a solid food, on composition and system kinetic, *i.e.*, changes over temperature and time[20]. Previous studies found a compositional dependence of S values in solid foods, which refers to the overall mobility of the system that can be derived from the mobility of individual components[19]. Therefore, such compositional dependence of the S value would give a possible approach for revealing the fundamental role that water plays in solid foods. However, the quantification of water mobility in solid foods still lacks study as the fundamental aspects of compositional dependence of S still needs to be discussed and extended by considering the application of classical thermodynamics.

Glucose, a commonly used food ingredient, often presents in glass formers and readily crystallizes owing to its hydrophilic and nonequilibrium nature[21]. Whey protein isolates (*WPI*), which can effectively prevent

the phase and state transition of glassy compounds, is widely added into food as a commercial stabilizer in the industry[22]. In this study, the glucose and *WPI* were chosen to composite solid-food model after lyophilizing, and the *Debaryomyces hansenii* (*D. hansenii*) was chosen as a target microorganism and inoculated in the glucose/ *WPI* solid matrices for incubating 36 hours at $a_w \geq 0.76$ and 30 ºC. The water sorption and thermodynamic properties of amorphous glucose/ *WPI* solid matrices were measured after equilibrium at various a_w and 30 ºC, whilst the thermodynamic discussion was complemented in explicating the composition dependence of *S*. The mobility difference between system-involved water and liquid pure water was calculated and gave a definition of an innovative indicator: water usability, U_w. The potential usage of water usability in modulating microbial growth was also investigated by relating U_w values to the growth characteristics of *D. hansenii*. In this paper, the proposed U_w, which contributed to a combinative parameter of thermodynamic properties and water mobility dynamics, can better understand the water relationships of microorganisms in low-moisture food preservation.

Materials And Methods

5.1. Food model preparation

α-D-Glucose (Crystals; Sigma Aldrich, St. Louis, USA) and *WPI* (Powder; carbohydrates or lipids as impurities < 10 ; Mullins Whey Inc., Mosinee, USA) were used to composite the food model. The glucose and *WPI* solutions (20, w/w) were prepared separately in deionized water and subsequently mixed to obtain solutions at different mass ratios (7:3, 1:1, 3:7, and 0:1; w/w). Further, the 5 *mL* of prepared solutions, loaded in preweighed 20 *mL* glass vials (semi-closed), were frozen in a still-air freezer (DW-HL240, Zhongkemeiling Co., Ltd., China) at − 20°C for 24 h, and then, were subsequently tempered at − 80°C for 3 h prior to lyophilization. The amorphous samples were obtained until the chamber pressure in a laboratory-used freeze dryer (10N/B, Scientz, Ningbo, China) was below 2 bar. It should note that lyophilizing glucose is extremely difficult due to its low T_g and high solubility nature[21]. In this study, therefore, the amorphous glucose was obtained experimentally via a modified quench-cooling approach reported by Simperler and Others[23], in which approximately 1 g of glucose crystals was cooled to − 30°C and melted at 160°C, and then, quench-cooled again to − 30°C. Three units of each amorphous sample were stored in vacuum desiccators over desiccant (P_2O_5; Sigma-Aldrich, St. Louis, USA) to avoid water sorption and reach equilibrium at 30°C for further analysis.

5.2. Water sorption testing

The amorphous samples were weighed to monitor water sorption behavior as a function of time (24 h intervals until 120 h) over saturated solutions of *LiCl*, CH_3COOK, $MgCl_2$, K_2CO_3, $Mg(NO_3)_2$, $NaNO_2$, and *NaCl* (Sigma Aldrich, St. Louis, Mo., USA) at respective a_w of 0.11, 0.20, 0.31, 0.43, 0.53, 0.65, and 0.75 at storage temperature of 30°C, in vacuum desiccators. The *Guggenheim-Anderson-de Boer* (GAB) model (Eq. 1) was applied to fit the water sorption data of each sample, where the m and m_0 referred to the weighted water content and monolayer water content; C_{GAB} and K_{GAB} were constants[24].

$$\frac{\mathrm{m}}{\mathrm{m}_0}=\frac{\mathrm{C}_{\mathrm{GAB}}\mathrm{K}_{\mathrm{GAB}}\mathrm{a}_{\mathrm{w}}}{(1-\mathrm{K}_{\mathrm{GAB}}\mathrm{a}_{\mathrm{w}})(1-\mathrm{K}_{\mathrm{GAB}}\mathrm{a}_{\mathrm{w}}+\mathrm{Cka}_{\mathrm{w}})}$$

1

5.3. Thermal Analysis

The thermal properties, including the onset-T_g value for each sample, were determined using a differential scanning calorimeter (*DSC*; Mettler-Toledo, Schwerzenbach, Switzerland). About 15 mg of prepared samples were transferred into a pre-weighed 50 mL aluminum pan and hermetically sealed before measurement. An empty punctured pan was used as a reference to minimize the systematic error caused by water vapor. Samples were scanned from − 20°C to over the T_g region at 5°C /min and then cooled at 10°C /min to the initial temperature. A second heating scan was run to well above the T_g at 5 °C/min. The onset-T_g derived from second heating scans were recorded using STARe software (Version 8.10, Mettler-Toledo, Schwerzenbach, Switzerland). The *Gordon-Taylor* (*GT*) equation (Eq. 2) had proven to fit experimental onset-T_g data of glucose/ *WPI* solid matrices, where w_1 and w_2 were the mass fractions of amorphous sample and water, T_{g1} and T_{g2} were their values, and k_{GT} was a constant and its thermodynamic meaning discussed later.

$$\frac{\mathrm{W}_2}{\mathrm{T}_{\mathrm{g}}-\mathrm{T}_{\mathrm{g2}}}=\mathrm{k}_{\mathrm{GT}}\mathrm{w}_1\left(\mathrm{T}_{\mathrm{g}}-\mathrm{T}_{\mathrm{g1}}\right)$$

2

5.4. Dynamic-Mechanical Analysis

The mechanical properties of prepared samples were studied by using a dynamic-mechanical analyzer (*DMA*; Mettler-Toledo, Schwerzenbach, Switzerland). The loss modulus (*E″*) of materials as a function of temperature at different frequencies (0.5, 1, 3, 5, and 10 *Hz*) were determined in this study. Before starting an experiment, the instrument was balanced and set at zero to determine the zero-displacement position and return the force to the zero position. Approximately 100 mg samples of ground materials were spread on a titanium pocket-forming sheet. The length, width, and thickness (~ 2 mm) of the sample pocket between the clamps were measured. Samples were scanned from − 20 °C to over the T_g region with a cooling rate of 5 °C/min and a heating rate of 2 °C/min using the single cantilever bending mode to obtain *E″* values using *DMA* software (Version 1.43.00, Mettler-Toledo Schwerzenbach, Switzerland). During heating, the samples were analyzed for T_a values determined from the peak temperature of *E″*[25].

5.5. Molecular mobility determination

The temperature difference (T_a–T_g), at which relaxation times (τ) exceed time factors critical to the characteristics of the materials, was used to calculate *S* values, which can represent the extent of molecular mobility as noted above. The τ and the temperature of T_a above T_g were modeled and analyzed using the *William-Landel-Ferry* (*WLF*) equation (Eq. 3), where T, T_g, τ, τ_g, refers to the experiment

temperature, onset-T_g, experimental *a*-relaxation time (oscillation frequency set in *DMA* measurement, τ = ½π*f*), and relaxation time in glass state (≈ 100 s). The *WLF* model constants C_1 and C_2 can be derived from a plot of $1/\log(\tau/\tau_g)$ against $1/(T_a-T_g)$ using experimental τ with the assumption of τ_g = 100 s at the onset-T_g[20]. Moreover, the *S* value of the system is determined by Eq. (4), where C_1, C_2, and d_s refers to the material-special *WLF* constants and the decrease in the number of logarithmic decades for τ (which d_s = 4), respectively.

$$\mathrm{Log}\left(\frac{\tau}{\tau_{\mathrm{g}}}\right)=\frac{-\mathrm{C}_1(\mathrm{T}-\mathrm{T}_{\mathrm{g}})}{\mathrm{C}_2+(\mathrm{T}-\mathrm{T}_{\mathrm{g}})}$$

3

$$\mathrm{S}=\frac{\mathrm{d}_{\mathrm{s}}\mathrm{C}_2}{-\mathrm{C}_1-\mathrm{d}_{\mathrm{s}}}$$

4

Previous studies reported that the compositional dependent of *S* in non-crystalline sugar/protein solids could be represented by Eq. (5). Where w_1 and w_2 referred to the mass fractions of dry solids and water, k_{sp} was a partition constant of molecular mobility, S_{d1} and S_{d2} represented the *S* value for anhydrous solids and amorphous water[26].

$$\mathrm{S}_{\mathrm{p}}=\frac{\mathrm{w}_1\mathrm{S}_{\mathrm{d1}}+\mathrm{k}_{\mathrm{sp}}\mathrm{w}_2\mathrm{S}_{\mathrm{d2}}}{\mathrm{w}_1+\mathrm{k}_{\mathrm{s}}\mathrm{w}_2}$$

5

5.6. Microbial response determination

Yeast Activation The *D. hansenii* (ACCC 20010; Xuanya Biotechnology Co. Ltd., China), isolated from the natural microflora, was chosen as a targeting microorganism because of its xerotolerant nature. *D. hansenii* was activated prior to inoculation on the bases of the method reported by Sharma and Others[27]. The lyophilized strains were dissolved and inoculated in a glassy tube containing 0.5 mL liquid *YM* agar (2.0% glucose, 0.5% yeast extract, 1.0% *NaCl*, 0.23% NaH_2PO_4, 0.5% $(NH_4)_2SO_4$, and 1.8% agar; Sartorius Stedim Biotech, Globaltec Corp., Germany) at 30°C on a rotational shaker (200 rpm) for 24 h, and the successful activation achieved when the single colony was obtained.

Sample Inoculation The lyophilized sample were stored in vacuum desiccators over P_2O_5 as a desiccant to avoid water sorption and used *UV* light was for 24 h to eliminate environmental effects prior to inoculation. A tiny quantity of yeast-containing solution (~ 0.2 *µl*) was streaked on amorphous glucose/ *WPI* solid matrices at mass rations of 1:0, 7:3, 1:1, 3:7, and 0:1. The inoculated glucose/ *WPI* solid matrices were rehumidified over a saturated solution of *NaCl*, *KCl*, and K_2SO_4 (Sigma Aldrich, St. Louis, Mo., USA) at respective a_w of 0.75, 0.83, and 0.92 a_w at 30°C, respectively. Previous studies have

verified that the low proportion of water incorporated with the inoculation did not raise the water content of the sample at a_w > 0.75[8]. Other equilibrated samples were not inoculated, but rather placed in a closed container over studied storage a_w ranges and temperature for blank control. It is important to know that the whole inoculation was implemented in a clean bench, which can maintain a sterilized condition to avoid contamination from the surrounding ambient.

Growth Characterization Scanning electron microscopy (*SEM*; Phenom Pro, Phenom World. BV, Holland) was used to observe the morphology of microbes in glucose/ *WPI* solid matrices at an acceleration voltage of 10 *KV*. The studied samples were coated using a gold-palladium alloy coater (Baltec Co., Manchester, NH) and observed at 8000 × magnification. Built-in instrument software (SEM Center, JEOL, Japan) was used for image collection. The growth characters of *D. hansenii* in the glucose/ *WPI* solid matrices were determined by an *ATP* fluorescence detector (*Pi-102*, Hygiena, USA) at 3 h intervals for 36 h and plotted the growth curve thereafter. The specific growth rate value of the *D. hansenii* in each system was determined by Eq. (6), and the cell doubling time of each system could be determined by Eq. (7). Where μ was the growth rate (h^{-1}), g was cell doubling time (h), N_0 is the number of microbial cells at the beginning, N_t is the number of microbial cells at any time, and t is time (h).

$$\mu = \frac{(lnN_t - lnN_0)}{t}$$

6

$$\mathrm{g}=\frac{ln\,(2)}{\mu}$$

7

5.7. Statistical Analysis

The *GAB* isotherms and *GT* equation, *S* parameter, and microbial growth characteristics of triplicate measurements were analyzed and plotted in Microsoft Excel (2019, Microsoft, Inc., USA). The average values with a standard deviation of triplicate measurements were calculated. Additionally, the error bars and significance analysis were implemented in the confidence interval of 95% to represent the variability of data.

Results And Discussion

2.1. Water sorption isotherms

The steady-state water sorption data and corresponding sorption isotherms for prepared glucose/ *WPI* solid matrices (1:0, 7:3, 1:1, 3:7, and 0:1; *w/ w*) after equilibrium at various storage conditions (0.11 ~ 0.76 a_w at 30 ºC) were shown Fig. (1) and given in *Supplementary material*. The water sorption data of each sample was slightly lower than previous reports, probably owing to the variation in the dehydration

process, sorption time, and storage temperature[28]. In this study, the crystallization of amorphous glucose was observed as sorption data rapidly decreased after 12 h of storage at all studied a_w and 30 ºC (Fig. 1a). This was caused by the non-crystallized portion rejected sorbed water molecules from glucose crystals formation, which induced desorption behavior[24]. No water release was found in glucose/*WPI* matrices with studied mass ratios at a_w below 0.44 and 30 ºC, whereas the lost of sorbed water was observed and slightly became rapid in glucose/WPI with 7:3 and 1:1 (w/w) at a_w above 0.44 (Fig. 1b to *d*). This result was induced by the *WPI*-derived physical-blocking effects reduced molecular diffusion, then, induced the partial crystallization of amorphous glucose. However, the high a_w condition might weaken crystallization owing to a water mobility-driven plasticization[29]. Moreover, crystallization was merely observed in pure *WPI* over the whole studied a_w range at 30 ºC during 120 h of storage (Fig. 1e). In this study, the water sorption data in glucose/*WPI* solid matrices exhibited a result of fractional quantities at $a_w \leq 0.44$ and 30°C, whilst he *GAB*-derived monolayer sorption (m_0) value of glucose/*WPI* solid matrices showed composition-dependent characteristic (Fig. 1f). This indicated that the phase separation occurred in glucose/*WPI* matrices during water sorption testing, where water was individually hydrogen bonding to protein and glucose; thus, fewer hydrogen bonds might exist between protein and lactose in mixtures[30]. Potes and Others[25] have reported a water additive principle in sugar/protein solid matrices, which refers to the steady-state water content of non-crystalline sugar that could be calculated through pure protein and high protein-containing systems based on phase separation and *GAB* sorption isotherms (Eq. 8). Where, W_t is the total equilibrium water content in the system; $n_1, \cdots, n_n$ is the mass fraction of each component in the system; $W_1, \cdots, W_n$ is the water contents sorbed by each component. Therefore, the steady-state water contents for non-crystalline glucose from 0.11 to 0.75 a_w and glucose/*WPI* solid matrices (7:3 and 1:1, w/w) from 0.52 to 0.75 a_w were calculated and given in *Supplementary Material*. Since glucose is a readily crystallizable biomaterial due to its low T_g and high solubility nature, the above finding and calculated sorption data for non-crystalline glucose in sugar/protein solid matrices have great importance in the development of processing and shelf-life control procedures for glucose-containing solid foods.

$$W_t = n_1 W_1 +, \cdots, + n_n W_n$$

8

2.2. Thermodynamic Properties

Thermal Properties The calorimetric onset-T_g values of glucose/*WPI* solid matrices (1:0, 7:3, 1:1, 3:7, and 0:1; *w/w*) after storage at $a_w \leq 0.44$ and 30°C determined by *DSC* were given in Table (1). In this paper, the T_g values of amorphous glucose were agreed with Simperler and Others[23], and a slightly difference may be found in sample preparation, environmental factors, or measurement methods. At the high a_w range (≥ 0.54 a_w), it was not easy to measure the T_g value of each sample due to the crystallization occurring, and T_g was not observed in pure *WPI* because the vitrification transformation of protein was not obvious. It should note that the glass transition occurred only in non-fatty solid components and was

affected by water-mobility-induced plasticization[29]. In Table (1), hence, the T_g value of the systems with higher *WPI* content was higher than pure glucose at studied conditions, which because of the stronger water binding ability of *WPI* may weak the mobility of water. The relationship between T_g values and water content (Dry ~ 0.44 a_w) of glucose/*WPI* solid matrices (1:0, 7:3, 1:1, and 3:7, *w/w*) was correlated by *GT* model (Eq. 2) and shown in Fig. (2*a*). The T_g data of non-crystalline samples were calculated by applying the extrapolating water sorption data from *GAB* isotherms into *GT* model. It should note that the k_{GT} in *GT* model was related to the strength of interaction between components in the mixture, namely hydrogen bond and charge transfer interaction, which could be calculated by the mass fraction of sorbed water in the glucose/*WPI* solid matrices[24]. In Fig. (2*a*), similarly, the k_{GT} value increased with the increase of *WPI* content in the system. This result indicated that the mobility of water molecules was captured or trapped by the presence of protein via water-bonding sites, and *WPI* could disturb the mobility of water in glucose/*WPI* solid matrices in agreement with water sorption results.

Mechanical Properties Fig. (2*b* to *e*) showed the *DMA* spectrum (*E″* peak frequency is 0.5 Hz) of studied glucose/*WPI* solid matrices (1:0, 7:3, 1:1, 3:7, and 0:1; *w/w*) after storage at $a_w \leq 0.44$ and 30°C determined by *DMA*. In the experimental temperature range, the *E″* peak of glucose decreased and widened with the decrease of a_w, which was caused by the change of dynamic-mechanical properties of amorphous materials affected by water, and the changes in water content could change the molecular mobility of solid matrices, and thus, interfering with the peak of *E″* in multi-frequency testing mode. At $a_w \leq 0.44$ and 30°C, the *E″* peak intensity of glucose/*WPI* matrices decreased with the increase of *WPI* content. The above result suggests that water mobility-induced plasticization in studied solid matrices could be disturbed by the presence of proteins, as noted above. The peak temperature of *E″* was used to determine the T_α of the mixture (Table 1). The T_α referred to the temperature point at which the mobility of amorphous sugar molecules was inphase with a certain frequency[25]. In this study, the T_α of glucose/*WPI* solid matrices decreased with the increase of a_w, while the increase of *WPI* content could increase the T_α value of the system (Table 1). The physical state of the mixture system was strongly affected by the water content, which changed the molecular mobility of glucose and disrupted T_α. According to *DMA* results, therefore, the mobility of water could affect the molecular interactions, α-relaxation, and T_α of solid foods.

Table 1
The calorimetric onset-T_g, T_a, *WLF*-constant C_1 and C_2, and S value for glucose/WPI solid matrices (1:0, 7:3, 1:1, 3:7, and 0:1; *w/w*) after equilibrium at studied a_w and 30 ℃.

		a_w	T_g (℃)	T_a (℃)	C_1	C_2	S (℃)
Glucose	Pure	Dry	38.2 ± 1.1*	54.2 ± 2.8a**	-0.3 ± 1.7a	-18.1 ± 3.6a	16.9 ± 1.6a
		0.11 ± 0.01	34.6 ± 3.2a	44.1 ± 3.1b	-3.6 ± 5.3b	-16.2 ± 4.3b	15.0 ± 4.7b
		0.20 ± 0.03	30.8 ± 4.4b	33.7 ± 2.5c	6.5 ± 2.8c	7.9 ± 3.7c	12.6 ± 2.2c
		0.31 ± 0.01	25.5 ± 2.8c	28.2 ± 5.1d	-0.9 ± 3.7d	-10.8 ± 4.5d	8.6 ± 1.3d
		0.42 ± 0.02	12.4 ± 4.2d	-	-	-	6.7 ± 2.4***
		0.52 ± 0.05 0		-	-	-	5.1 ± 4.5
		0.62 ± 0.01		-	-	-	4.6 ± 3.1
		0.75 ± 0.02		-	-	-	3.0 ± 1.7
		0.81 ± 0.03		-	-	-	2.1 ± 1.2
		0.92 ± 0.04		-	-	-	1.6 ± 1.5
		1.00 ± 0.08		-	-	-	1.5 ± 1.2
Glucose/WPI	7:3	Dry	56.5 ± 2.4a	80.3 ± 4.7a	-5.9 ± 1.6a	-81.5 ± 3.7a	31.3 ± 0.8a
		0.11 ± 0.01	45.4 ± 3.4b	67.6 ± 5.3b	-1.5 ± 2.5b	-25.9 ± 4.7b	25.2 ± 1.2b
		0.20 ± 0.03	33.2 ± 3.1c	66.8 ± 3.5c	5.6 ± 3.4c	18.9 ± 3.1c	19.4 ± 2.5c
		0.31 ± 0.01	24.9 ± 2.3d	30.2 ± 2.4d	8.3 ± 4.7d	16.2 ± 1.9d	11.5 ± 0.9d

*: Values are means ± SDs (n = 3); **: significant analysis at $p<0.05$; ***: The prediction S value.

		a_w	T_g (℃)	T_a (℃)	C_1	C_2	S (℃)
		0.42 ± 0.02	16.5 ± 3.6[e]	26.7 ± 4.2[e]	-1.8 ± 3.7[e]	-8.5 ± 1.2[e]	7.5 ± 1.4[e]
		0.52 ± 0.05 0		-	-	-	5.6 ± 3.3
		0.62 ± 0.01		-	-	-	4.1 ± 2.5
		0.75 ± 0.02		-	-	-	3.4 ± 2.2
		0.81 ± 0.03		-	-	-	2.5 ± 0.9
		0.92 ± 0.04		-	-	-	1.8 ± 1.3
		1.00 ± 0.08		-	-	-	1.6 ± 2.1
Glucose/WPI	1:1	Dry	70.9 ± 2.2[a]	85.4 ± 3.1[a]	-6.5 ± 4.7[a]	-36.7 ± 2.9[a]	38.7 ± 2.5[a]
		0.11 ± 0.01	52.6 ± 1.5[b]	62.4 ± 4.6[b]	-4.5 ± 3.8[b]	-29.9 ± 4.3[b]	29.2 ± 0.8[b]
		0.20 ± 0.03	44.0 ± 2.8[c]	45.5 ± 5.8[c]	-6.8 ± 5.1[c]	-35.6 ± 6.4[c]	20.4 ± 1.0[c]
		0.31 ± 0.01	34.2 ± 3.0[d]	42.3 ± 3.7[d]	9.6 ± 4.7[d]	25.6 ± 2.3[d]	17.5 ± 2.6[d]
		0.42 ± 0.02	22.1 ± 4.3[e]	32.9 ± 4.5[e]	-3.8 ± 1.1[e]	-13.7 ± 2.8[e]	12.9 ± 3.1[e]
		0.52 ± 0.05 0		-	-	-	11.1 ± 3.2
		0.62 ± 0.01		-	-	-	9.3 ± 0.5
		0.75 ± 0.02		-	-	-	7.6 ± 1.5
		0.81 ± 0.03		-	-	-	6.4 ± 2.1

*: Values are means ± SDs (n = 3); **: significant analysis at $p<0.05$; ***: The prediction S value.

		a_w	T_g (℃)	T_a (℃)	C_1	C_2	S (℃)
		0.92 ± 0.04		-	-	-	5.1 ± 3.8
		1.00 ± 0.08		-	-	-	5.3 ± 2.5
Glucose/WPI	3:7	Dry	93.2 ± 1.2[a]	88.1 ± 4.5[a a*]	-0.1 ± 0.8[a]	-41.1 ± 0.6[a]	41.7 ± 1.5[a]
		0.11 ± 0.01	83.1 ± 2.1[b]	80.1 ± 2.8[b]	-9.6 ± 1.4[b]	-38.1 ± 5.7[b]	37.6 ± 2.2[b]
		0.20 ± 0.03	59.1 ± 4.1[c]	68.2 ± 1.9[c]	-7.4 ± 2.8[c]	-29.4 ± 2.9[c]	27.9 ± 1.9[c]
		0.31 ± 0.01	50.1 ± 2.0[d]	59.7 ± 4.4[d]	-6.7 ± 2.7[d]	-62.4 ± 5.2[d]	23.4 ± 3.1[d]
		0.42 ± 0.02	33.8 ± 3.0[e]	40.9 ± 5.3[e]	-5.5 ± 1.8[e]	-21.6 ± 7.2[e]	20.5 ± 0.9[e]
		0.52 ± 0.05 0		-	-	-	18.3 ± 1.2
		0.62 ± 0.01		-	-	-	16.7 ± 2.5
		0.75 ± 0.02		-	-	-	15.0 ± 3.0
		0.81 ± 0.03		-	-	-	14.4 ± 0.5
		0.92 ± 0.04		-	-	-	13.8 ± 1.1
		1.00 ± 0.08		-	-	-	6.5 ± 1.1

*: Values are means ± SDs (n = 3); **: significant analysis at $p<0.05$; ***: The prediction S value.

Table 2
The specific growth rate (μ) and cell doubling time (g) of *D. hansenii* in glucose/*WPI* solid matrices (7:3, 1:1, 3:7, and 0:1, *w/w*) after storage at 0.75 ~ 0.92 a_w and 30 ºC for 36 hours.

a_w		glucose/*WPI* 7:3	glucose/*WPI* 1:1	glucose/*WPI* 3:7	glucose/*WPI* 0:1
0.75 ± 0.02	μ (h^{-1})	0.0430 ± 0.0423[a*]	0.0506 ± 0.0548[a]	0.0529 ± 0.0045[a]	0.0531 ± 0.0521[a]
	g (h)	23.2548 ± 0.2462[A**]	19.8073 ± 0.0231[A]	18.9199 ± 0.1213[A]	18.8173 ± 0.0251[A]
0.81 ± 0.03	μ (h^{-1})	0.0489 ± 0.0655[b]	0.0530 ± 0.0137[b]	0.0572 ± 0.0213[b]	0.0577 ± 0.0125[b]
	g (h)	20.4584 ± 0.3231[B]	19.2197 ± 0.0152[B]	17.4873 ± 0.4463[B]	17.3128 ± 0.2657[B]
0.92 ± 0.04	μ (h^{-1})	0.0556 ± 0.0264[c]	0.0607 ± 0.0765[c]	0.0614 ± 0.0321[c]	0.0697 ± 0.0216[c]
	g (h)	17.9829 ± 0.4655[C]	16.4681 ± 0.4355[C]	16.3722 ± 0.5418[C]	14.3465 ± 0.2651[C]

*: Significant analysis at p<0.05;

**: Values are means ± SDs (n = 3).

2.3. Molecular Mobility Measurement

In Fig. (3*a* to *d*), the relationship between *DMA*-derived α-relaxation time (τ) and temperature difference ($T_g - T_a$) for studied glucose/*WPI* solid matrices (1:0, 7:3, 1:1, and 3:7; *w/w*) that equilibrium at low a_w (dry ~ 0.44 a_w) and 30°C was successfully fitted by *WLF* equation (Eq. 3) with materials-specific constants C_1 and C_2. It should note that the *WLF* constants C_1 and C_2 often involve different physical meanings for describing solids flow characteristics, where C_1 is a time factor that refers to the maximum number of log decades for the change in τ as anchored to T_g and C_2 expresses a theoretical temperature (°C) for infinite τ[24]. Most of the *WLF* relationships for studied solid matrices showed down concavity as their C_1 and C_2 values were numerical negative, which both increased concomitantly with a_w increases (Table 1). This resulted from the water mobility-induced plasticization that could decrease the T_g of solid systems, where τ rapidly dropped in several logarithmic decades when the temperature was above T_g. It should note that the determination of τ in relaxation data measured at different frequencies by *DMA* can refer to the time factor corresponding to the material response to a change in internal or external thermodynamic conditions such as temperature and a_w, which can provide a new approach for the description of the mobility dynamics for food constituents[13]. Previous studies reported a *WLF* constant derived *S* concept

was a measurement of structural transformation and mobility resistance, which could be used to determine the molecular mobility of solid foods[20]. In this study, the *S* values of the glucose/*WPI* solid matrices (1:0, 7:3, 1:1, and 3:7; *w*/*w*) increased with the increase of *WPI* content but decreased with a_w increases (Table 1). This indicated that water mobility-induced plasticization could reduce the T_g and increase the apparent molecular mobility of the system, whereas the presence of *WPI* delayed the apparent molecular mobility owing to its physical blocking effects and water bonding sites reduced the mobility of sugar and water molecules. Previous studies have proposed a practical equation (Eq. 5) to describe the relationship between water content and *S* in amorphous sugar/protein systems[19]. The such the relationship was also applied for describing the influence on numerical *S* values and water content of glucose/*WPI* solid matrices and achieved an excellent fitting performance in this paper (Fig. 3e to *h*). The present work confirms that the *Strength* approach is universal and can apply to hygroscopic monosaccharides/protein systems, which possess a practical potential in the fabrication of dampproof foods as well as improving the processability, quality, and shelf-life of solid foods.

2.4. Mobility dynamics of water

Thermodynamic discussion The constant k_{sp} in Eq. (5) implies the extent of water mobility-induced plasticization on amorphous food systems, in which a small k_{sp} refers to a less strong structure[24]. In this study, similarly, the constant k_{sp} of studied glucose/*WPI* solid matrices were increased by the presence of *WPI* owing to the extent of plasticization was weakened by protein. Despite the compositional dependence of *S* values in Eq. (5), the k_{sp} of studied samples were very similar but only slightly higher than the *GT* constant k_{GT}, numerically (Fig. 2a & Fig. 3e to *h*). Although k_{sp} and k_{GT} were respectively calculated on the basis of the T_g and mobility dynamics, their numerical similarity is not entirely coincidental. The thermodynamic discussion on the effects of composition on the *S* value in Eq. (5) and corresponding constant k_{sp} was carefully explicated below. For simplicity, the pure amorphous glucose was taken as an example, where the respective mole fractions of the two components (glucose and water) in the system are denoted as x_1 and x_2, C_{p1} and C_{p2} denote the molar heat capacities, and the molar entropies of these pure components are designated in turn as $\bar{S}_1$ and $\bar{S}_2$. The molar entropy ($\bar{S}_{mix}$) of the binary system can be written generally as $\bar{S}_{mix} = x_1\bar{S}_1 + x_2\bar{S}_2 + \Delta\bar{S}_{mix}$. Where the $\Delta\bar{S}_{mix}$ includes excess entropy (solely conformational for simplest case) changes associated with mixing the two components. Couchman and Karasz[31] have treated glass transition as an Ehrenfest second-order transition on the basis of the configurational entropy theory and used the thermodynamic characteristic continuity and discontinuity conditions, together with some simple explicit assumptions and approximations, to provide relations expressing the T_g of the binary mixture in terms of the T_{g1} and T_{g2} of the individual pure components. Based on the above assumption, the composition of the system is fixed it then follows that $\Delta\bar{S}_{mix}$ is continuous at T_g range, which pointed to a circumstance where the

character and extent of specific interactions barely changed at T_g as non-conformational contributions to the excess entropy of mixing. Therefore, the $\bar{S}_{mix}$ of the binary system can be written generally in Eq. (9). As noted above, the *S* parameter refers to an allowable temperature increase above the calorimetric onset-T_g for non-crystalline materials. Meanwhile, Slade and Others[11] have reported that the first-order transition for non-crystalline sugars, such as crystallization, was ~ 50 ºC above the calorimetric T_g value. In this study, we found that the *S* value for pure anhydrous glucose was 16.9 ºC above its calorimetric onset-T_g, whilst the presence of water decreased the *S* value of amorphous glucose (Table 1). This result proved that the *S* should locate in the Ehrenfest second-order transition range, which indicated the assumption suggested by Couchman and Karasz[31] can still hold to explain the compositional dependence of the *S* parameter. Therefore, let *T*, T_1 and T_2 denote temperature points above the calorimetric onset-T_g for the system and pure individual components within respectively glass transition range (T_g, T_{g1} and T_{g2}). The part of total molar entropy (Eq. 9), excluding excess entropy could be written generally as Eq. (10), where S_p, S_1, and S_2 refer to the *S* parameters for the binary system and involved components.

$$\bar{S}_{mix} = x_1 \left[\bar{S}_1 + \int_{T_{g1}}^{T_g} \frac{C_{p1}}{T} dT \right] + x_2 \left[\bar{S}_2 + \int_{T_{g2}}^{T_g} \frac{C_{p2}}{T} dT \right]$$

9

$$\bar{S}_{mix} = x_1 \left[\bar{S}_1 + \int_{T_1 - T_{g1}}^{T - T_g} \frac{C_{p1}}{T} dT \right] + x_2 \left[\bar{S}_2 + \int_{T_2 - T_{g2}}^{T - T_g} \frac{C_{p2}}{T} dT \right]$$

10

$$= x_1 \left[\bar{S}_1 + \int_{S_1}^{S_p} \frac{C_{p1}}{T} dT \right] + x_2 \left[\bar{S}_2 + \int_{S_2}^{S_p} \frac{C_{p2}}{T} dT \right]$$

10

Eq. (10) can be obtained for both the glassy and rubbery states, where the C_p undergoes a finite discontinuity at the transition[32]. Since $\bar{S}_1$ and $\bar{S}_2$ are continuous at respectively T_{g1} and T_{g2}, the continuity of $\bar{S}_{mix}$ at T_g, and the approximation that the transition isobaric heat capacity increments ΔC_{p1} and ΔC_{p1} are temperature independent provides the expression in Eq. (11). If the further approximation ln (1 + x) ≈ x is valid, the Eq. (11) was rearranged as Eq. (12), where the meaning of k_{sp} can also be written as the changes of heat capacities of individual components for the binary system. Consequently, the above classic thermodynamic discussion explicated that the k_{sp} and k_{GT} were not only similar in numerical value but shared the same thermodynamic meanings.

$$lnS_p = \frac{x_1 lnS_1 + \frac{\Delta C_{p2}}{\Delta C_{p1}} x_2 lnS_2}{x_1 + \frac{\Delta C_{p2}}{\Delta C_{p1}} x_2}$$

11

$$S_p = \frac{x_1 S_1 + \frac{\Delta C_{p2}}{\Delta C_{p1}} x_2 S_2}{x_1 + \frac{\Delta C_{p2}}{\Delta C_{p1}} x_2}$$

12

Water usability Although the thermodynamic discussion explicitly explains the thermodynamic meaning of k_{sp} and k_{GT}, their slight numerical difference is still unignorable and need to be clarified fully. In Fig. (3*e* to *h*), the extrapolation line for glucose/*WPI* solid matrices (1:0. 7:3, 1:1, and 3:7, w/w) were fitted by Eq. (5) using k_{GT} to replace k_{sp} as constant. In Fig. (3*e* to *h*), we noticed that the extrapolated *S* value by k_{GT} for water involved in solid matrices was higher than the extrapolated *S* value calculated by k_{sp}, which chose the literature *S* value from liquid pure water[19]. *Schmidt*[17] has pointed out that the overall mobility of water decreases when a component is added, and the magnitude of the decrease depends on the number, amount, and nature of the solute and processing methods based on *NMR* studies. Similarly, the water in solid matrices may exhibit different mobility dynamics than those of liquid pure water as the states of water in systems vary due to the hydrogen bonding, capillary, crystallized, *etc*. The varying mobility dynamic of water might contribute to fabricating the food structures and many other functional abilities for the whole systems, such as nutrients transportation, microbial growth, structural fabrications, and so on[33]. Therefore, the k_{GT} extrapolated *S* value could give a better description of the mobility dynamics of water involved in systems than the literature *S* value of liquid pure water. As noted above, the quantification of water mobility in solid foods requires considering both thermodynamic properties and water mobility dynamics. On the basis of the molecular mobility difference between water involved in solid matrices and liquid pure water in their T_g range, we introduced water usability (U_w) to give a measure for the mobility of water involved in solid matrices (Eq. 13). Where the S_1 and S_2 refers to the molecular mobility of liquid pure water and water involved in solids. Compared to a_w and T_g, the proposed U_w could give a better interpretation of the changes of water mobility in solid foods.

$$U_w = \frac{S_2}{S_1}$$

13

2.5. Microbial growth and U_w

Morphological characteristics The appearance of *D. hansenii* inoculated glucose/*WPI* solid matrices (7:3, 1:1, 3:7, and 1:0, w/w) after 36 h incubating at a_w varying from 0.75 to 0.92 a_w and 30°C were shown in

Fig. (4*a left*). It should note that none of *D. hansenii* could survive in pure glucose at all studied high a_w as the extreme osmotic pressure in this study, whereas the pure *WPI* solids would cultivate the *D. hansenii* as the impurities included in *WPI* powder might provide the growth factors for microbes. Previous studies reported that the presence of excess water surrounding the sugar/protein composite solids can create a continuous liquid phase allowing fast exchange among different regions of the sample as well as weakening the physical structure[34]. Similarly, the water sorption-induced structural collapse was observed in all studied glucose/ *WPI* solid matrices at mass ratios of 7:3, 1:1, and 3:7 after 36 h of incubating at a_w varying from 0.75 to 0.92 a_w and 30°C (Fig. 4a *left*). Besides, such morphological deterioration was also found in pure *WPI* solids, which disagreed with Fan and Roos[30] who pointed out that the amorphous protein might exhibit a stronger structure with no collapse phenomenon after equilibrium at a high a_w range. Based on the *SEM* observation, the colony of *D. hansenii* in glucose/ *WPI* solid matrices (7:3, 1:1, and 3:7, w/w) was found after 36 h of incubation at a_w varying from 0.75 to 0.92 a_w and 30°C, where the size of the strain increased with the increasing of *WPI* content (Fig. 4a *right*). Therefore, the *D. hansenii* that thrive in *WPI* solids could use the nutrients and release water through metabolisms, *e.g.*, glycometabolism and cellular respiration, thus, induce the structural collapse in pure *WPI* solids.

Microbial growth and U_w The growth characteristics of *D. hansenii* inoculated in glucose/ *WPI* solid matrices (7:3, 1:1, 3:7, and 0:1, w/w) were monitored in 36 h of incubation at a_w varying from 0.75 to 0.92 and 30°C by using *ATP* fluorescence detector (Fig. 4b to *d*). The growth rate (μ) and cell doubling time (g) of *D. hansenii* were calculated via Eqs. (6 and 7) and given in Table (2). The cell content of *D. hansenii* in glucose/ *WPI* solid matrices increased with the increase of *WPI* content that was consistency with *SEM* observation (Fig. 4b *to d*). This result indicated that the growth of *D. hansenii* was more vigorous as it entered the logarithmic growth phase earlier and rapidly reached the stable phase in a high protein-containing solids. Nevertheless, the tendency of the cell content for *D. hansenii* inoculated in glucose/ *WPI* solids was overlapped at studied a_w ranges (Fig. 4e). It is generally accepted that the tolerance and ability of xerophilic microbes to enable them to survive and grow at reduced a_w rely on a common approach, which indicated that the intracellular accumulation of compatible solutes, *e.g.*, glycerol, arabitol, and mannitol, to balance the a_w inside the cell against the external a_w[8]. Therefore, the microbial growth was highly dependent on the nature of the solutes and less dependent on a_w. Previous studies have reported that T_g is a physicochemical boundary to control microbial growth in low-moisture foods as the viscosity of the system increases as T_g increases[12,13]. For example, the decrease in solute mobility between glass-forming systems may affect the growth of *S. aureus* as the increasing of T_g, which in turn decreases the mobility of nutrients transportation and retards the metabolized activity[13]. However, increasing evidence have pointed out that the high viscosity can enhance the growth of microorganisms in the high-solid system as the slowing of diffusion rate by improving the T_g will making the system more stable and providing better nutrient sources for microorganisms[17]. These experimental findings implied that the growth of microorganisms seems not to correlate with the T_g and its-related viscosity variations of

media. Since the water mobility was highly correlated to many important diffusion-limiting processes for microbial growth and metabolic activity in low-moisture foods, in this study, the relationship between the U_w, μ, and g value of *D. hansenii* inoculated in glucose/*WPI* solid matrices (7:3, 1:1, 3:7, and 0:1; *w/w*) after incubation at 0.75 ~ 0.92 a_w and 30 ºC until 36 h were shown in Fig. (4*f to g*). The μ increased with the increase of the U_w value, whereas the g value decreased with the increasing of the U_w. This result indicated that the U_w is highly related to the survival and growth of microorganisms as the diffusant mobility was more necessary to support growth and metabolic activity rather than glassy solutes in low diffusion. Therefore, the mobility difference between water involved in foods and liquid pure water can provide a better understanding of the water relationships of microorganisms in low-moisture food preservation.

Conclusions

In this study, the water sorption isotherms, thermodynamic properties, molecular mobility, and microbial growth of glucose/*WPI* composite solid matrices were measured at various a_w and 30 ºC. Although the sorption isotherms, T_g, and relaxation processes of studied matrices were affected by a_w and *WPI*, the microbial growth showed highly dependent on water mobility rather than a_w. The mobility difference between the system-involved water and liquid pure water was explicated on the basis of a classical thermodynamic viewpoint, and water usability (U_w) was introduced to describe the dynamic changes of water mobility in glucose/*WPI* matrices. Despite to a_w, the microbial growth rate was enhanced at high U_w matrices concomitantly with the rapid cell doubling time. Therefore, the proposed U_w parameter, using the information of the dynamic changes of water mobility in a systematic manner, could quantify the water relationship of microorganisms in solid foods as well as have a practical meaning for modulating microbial growth of resultant products. Further research to assess the influence of U_w on growth parameters (*i.e.*, lag phase) and metabolic activity of mold and bacteria will be continually investigated in low-moisture food and pharmaceutical materials.

Declarations

4. ACKNOWLEDGMENTS

The authors thank Prof. Liqing Zhao and Miss Guiyun Zeng at the College of Chemistry and Environmental Engineering, Shenzhen University for their kindly help.TheNatural Science Foundation of Guangdong [Grant No.: 2022A1515011520], National Natural Science Foundation of China [Grant No.: 31801488], High-Level Talents Start-Up Funding of Shenzhen [Grant No.: 20180511594C], and The Government's Plan of Science and Technology (ZDSYS20210623100800001) are gratefully acknowledged.

6. DATA AVAILABILITY

The datasets generated during and/or analysed during the current study are available from the corresponding author on reasonable request.All data generated or analysed during this study are included in this published article [and its supplementary information files].

7. AUTHOR CONTRIBUTIONS

Tingting Cui Performed the research, Formal analysis, Resources, Data Curation.

Xukai Wu Performed the research, Writing – Original Draft, Data Curation.

Tian Mou Data Curation, Writing – Review and Editing.

Fanghui Fan, Dr. Conceptualization, Methodology, Writing – Review and Editing, Supervision, Funding Acquisition.

References

1. Panitsa, A., Petsi, T., Kandylis, P., Kanellaki, M., & Koutinas, A. A. Tubular Cellulose from Orange Juice By-Products as Carrier of Chemical Preservatives; Delivery Kinetics and Microbial Stability of Orange Juice. Foods. **10**(**8**), 1882 (2021).
2. Hameed, S., Xie, L., & Ying, Y. Conventional and emerging detection techniques for pathogenic bacteria in food science: A review. Trends Food Sci. Technol. **81**, 61–73 (2018).
3. Dao, H., Microbial stability of pharmaceutical and cosmetic products. Aaps Pharmscitech. **19**(**1**), 60–78 (2018).
4. Havelaar, A. H. et al. Future challenges to microbial food safety. Int. J. Food Microbiol. **139**, S79-S94 (2010).
5. Li, X., You, B., Shum, H. C., & Chen, C. H. Future foods: Design, fabrication and production through microfluidics. Biomaterials. **287**, 121631 (2022).
6. Tapia, M. S., Alzamora, S. M., & Chirife, J. (2020). Effects of water activity (aw) on microbial stability as a hurdle in food preservation. *Water Activity in Foods: Fundamentals and Applications* pp. 323–355 (Blackwell Publishing, UK, 2020).
7. Chitrakar, B., Zhang, M., & Adhikari, B. Dehydrated foods: Are they microbiologically safe?.CRIT REV FOOD SCI. **59**(**17**), 2734–2745 (2019).
8. Buera, M. P., Jouppila, K., Roos, Y. H., & Chirife, J. Differential scanning calorimetry glass transition temperatures of white bread and mold growth in the putative glassy state. *Cereal Chem.* **75**(**1**), 64–69 (1998).
9. Beuchat, L. R. et al. Low-water activity foods: increased concern as vehicles of foodborne pathogens. *J. Food Prot*. **76**, 150–72 (2013).
10. Igo, M. J., & Schaffner, D. W. Models for factors influencing pathogen survival in low water activity foods from literature data are highly significant but show large unexplained variance. Food

Microbiol. **98**, 103783 (2021).

11. Slade, L., Levine, H., & Reid, D. S. Beyond water activity: recent advances based on an alternative approach to the assessment of food quality and safety. Crit Rev Food Sci Nutr. **30**(**2–3**), 115–360 (1991).
12. Roos, Y. H. Glass transition temperature and its relevance in food processing. Annu Rev Food Sci Technol. **1**, 469–496(2010).
13. Stewart, C. M. et al. Staphylococcus aureus growth boundaries: moving towards mechanistic predictive models based on solute-specific effects. Appl. Environ. Microbiol. **68**(**4**), 1864–1871 (2002).
14. Chirife, J., Buera, M. P., & Gonzalez, H. L. The mobility and mold growth in glassy/rubbery substances. *Water Management in the Design and Distribution of Quality Foods* pp. 285–298 (CRC Press, Florida, 1999).
15. Lavoie, J. P., Labbe, R. G., & Chinachoti, P. Growth of Staphylococcus aureus as related to ^{17}O NMR water mobility and water activity. J. Food Sci. **62**, 861–866 (1997).
16. Kou, Y., Molitor, P. F., & Schmidt, S. J. Mobility and stability characterization of model food systems using NMR, DSC and conidia germination techniques. J. Food Sci. **64**, 950–959 (1999).
17. Schmidt, S. J. Water mobility in foods. *Water activity in foods: Fundamentals and Applications* pp. 61–122 (Blackwell Publishing, UK, 2020).
18. Li, R., Lin, D., Roos, Y. H., & Miao, S. Glass transition, structural relaxation and stability of spray-dried amorphous food solids: A review. Dry. Technol. **37**(**3**), 287–300 (2019).
19. Maidannyk, V. A., & Roos, Y. H. Water sorption, glass transition and “strength” of lactose–Whey protein systems. Food Hydrocoll. **70**, 76–87 (2017).
20. Fan, F., & Roos, Y. H. Structural relaxations of amorphous lactose and lactose-whey protein mixtures. J Food Eng. **173**, 106–115 (2016).
21. Makarem, N., Bandera, E. V., Nicholson, J. M., & Parekh, N. Consumption of sugars, sugary foods, and sugary beverages in relation to cancer risk: a systematic review of longitudinal studies. Annu. Rev. Nutr. **38**(**1**), 17–39 (2018).
22. Minj, S., & Anand, S. Whey proteins and its derivatives: Bioactivity, functionality, and current applications. Dairy. **1**(**3**), 233–258 (2020).
23. Simperler, A. et al. Glass transition temperature of glucose, sucrose, and trehalose: an experimental and in silico study. J. Phys. Chem. B. **110**(**39**), 19678–19684 (2006).
24. Cui, T., Wu, Y., & Fan, F. Physicochemical properties and Strength analysis of vitreous encapsulated solids for the safe delivery of β-Carotene. Food Res. Int. **151**, 110877 (2022).
25. Potes, N., Kerry, J. P., & Roos, Y. H. Additivity of water sorption, alpha-relaxations and crystallization inhibition in lactose–maltodextrin systems. Carbohydr. **89**(**4**), 1050–1059 (2012).
26. Wu, Y., Huang, W., Cui, T., & Fan, F. Crystallization and strength analysis of amorphous maltose and maltose/whey protein isolate mixtures. J. Sci. Food Agric. **101**(**6**), 2542–2551 (2021).

27. Sharma, P., Meena, N., Aggarwal, M., & Mondal, A. K. Debaryomyces hansenii, a highly osmo-tolerant and halo-tolerant yeast, maintains activated Dhog1p in the cytoplasm during its growth under severe osmotic stress. *Curr*. Genet. **48**(**3**), 162–170 (2005).
28. Hoobin, P. et al. Water sorption properties, molecular mobility and probiotic survival in freeze dried protein–carbohydrate matrices. Food Funct. **4**(**9**), 1376–1386 (2013).
29. Fan, F., Xiang, P., & Zhao, L. Vibrational spectra analysis of amorphous lactose in structural transformation: Water/temperature plasticization, crystal formation, and molecular mobility. Food Chem. **341**, 128215 (2021).
30. Fan, F., & Roos, Y. H. X-ray diffraction analysis of lactose crystallization in freeze-dried lactose–whey protein systems. Food Res. Int. **67**, 1–11 (2015).
31. Couchman, P. R., & Karasz, F. E. A classical thermodynamic discussion of the effect of composition on glass-transition temperatures. Macromolecules **11**(**1**), 117–119 (1978).
32. Zhou, D., Zhang, G. G., Law, D., Grant, D. J., & Schmitt, E. A. Physical stability of amorphous pharmaceuticals: importance of configurational thermodynamic quantities and molecular mobility. J Pharm Sci. **91**(**8**), 1863–1872 (2002).
33. Ding, S. et al. Peng, B., Li, Y., & Yang, J. Evaluation of specific volume, texture, thermal features, water mobility, and inhibitory effect of staling in wheat bread affected by maltitol. Food Chem. **283**, 123–130 (2019).
34. Vittadini, E., Dickinson, L. C., & Chinachoti, P. NMR water mobility in xanthan and locust bean gum mixtures: possible explanation of microbial response. Carbohydr. Polym. **49**(**3**), 261–269 (2002).

Figures

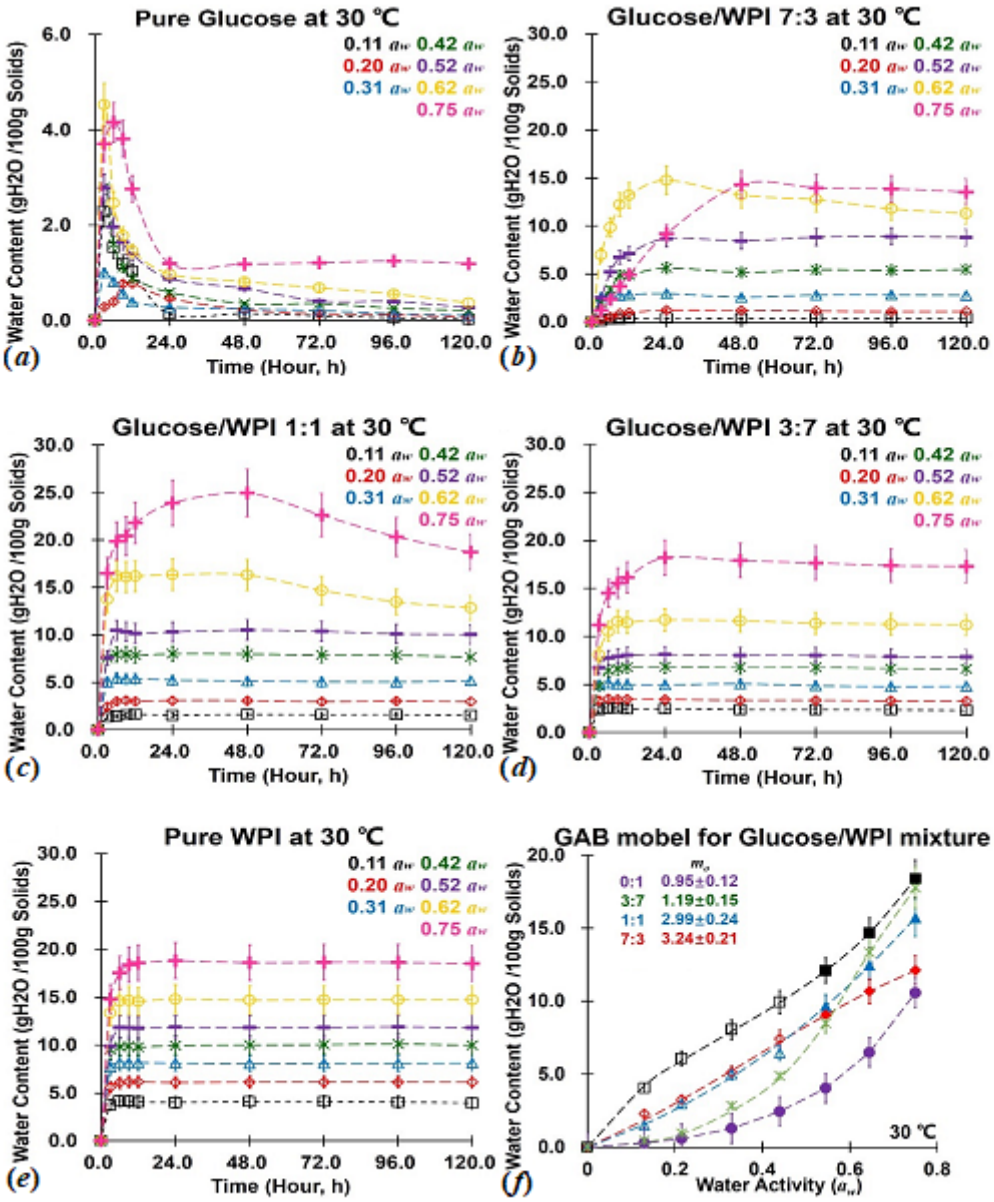

Figure 1

The water sorption isotherms for glucose/ *WPI* solid matrices with mass ratios of 1:0, 7:3, 1:1, 3:7 and 0:1 at a_w from 0.11 to 0.75 under 30 °C (*a* ~ *e*). The GAB model and monolayer sorption value (m_0) for each sample were given in (*f*), where the empty and solid symbols represent the experiment and calculated sorption data on the basis of Eq. (8), respectively.

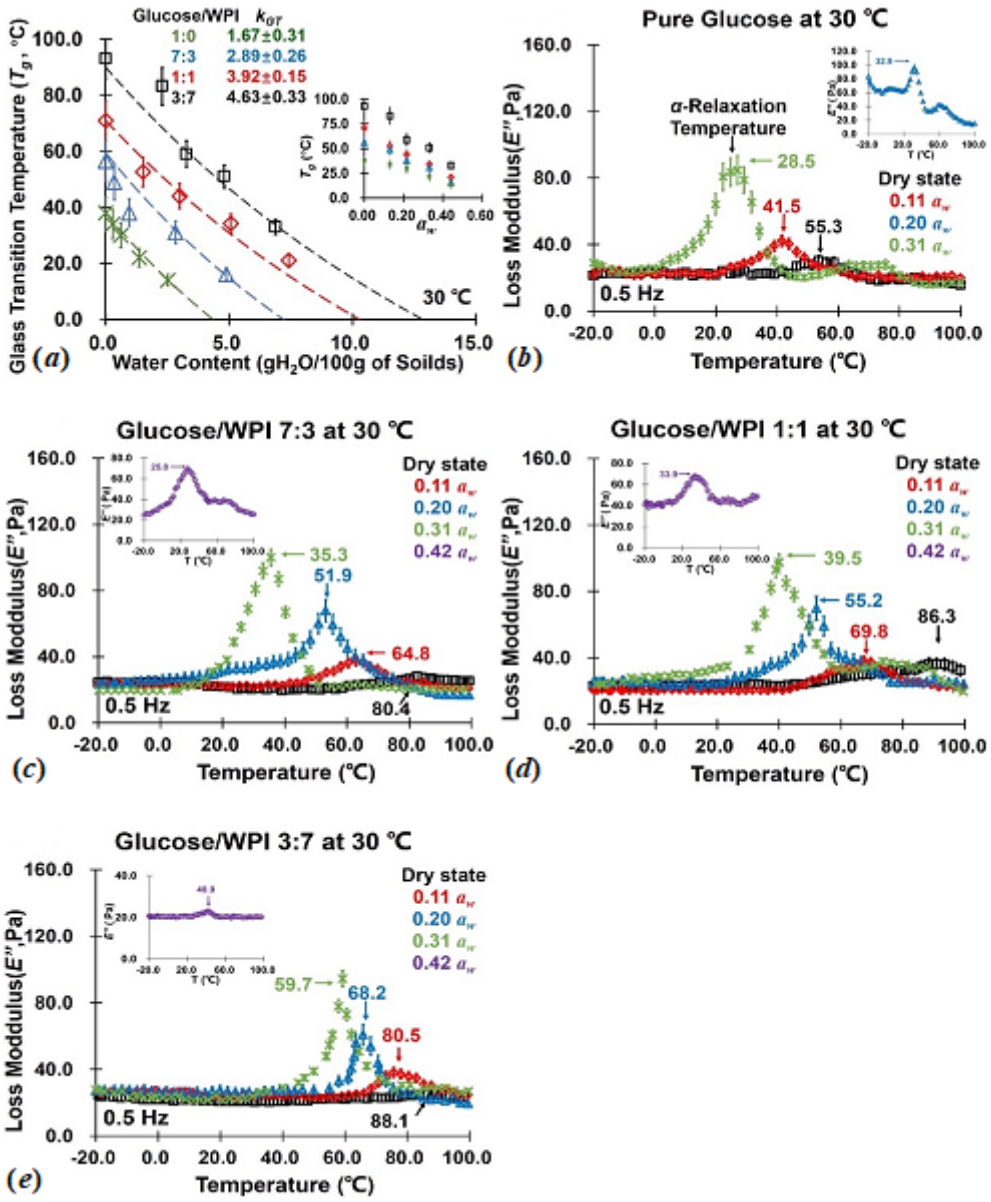

Figure 2

The calorimetric onset-T_g (*a*) and the *DMA* spectra of *E″* at 0.5 Hz (*b* to *e*) of glucose/WPI solid matrices (1:0, 7:3, 1:1, 3:7, and 0:1, *w*/*w*) stored from dry state to 0.44 a_w at 30 ºC. The T_g values against corresponding water sorption data were fitted by *GT* equation, and the T_a values were characterized from the peak temperature of *E″* (Potes *et al.*, 2012).

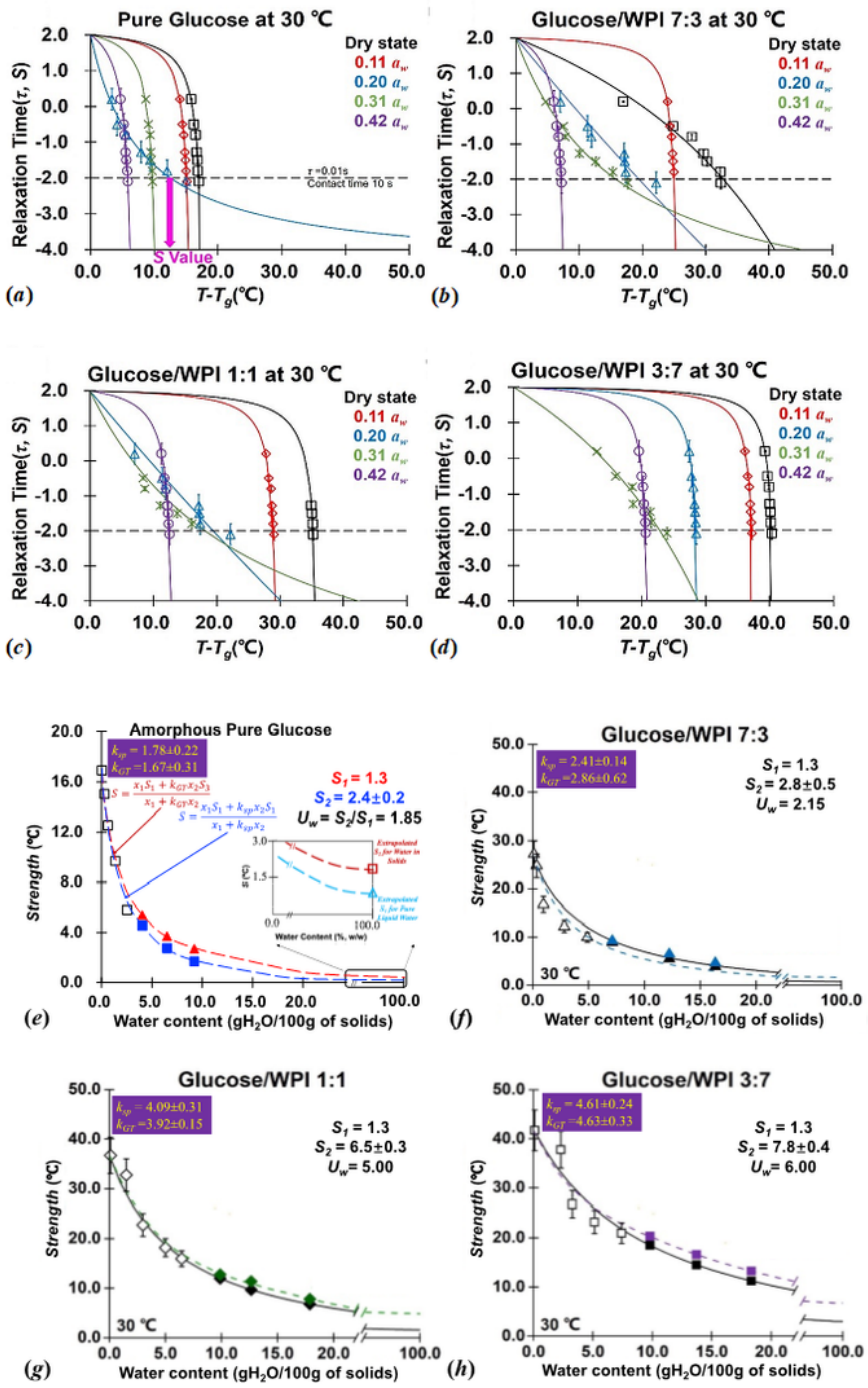

Figure 3

Strength (*S*) value for glucose/*WPI* solid matrices (1:0, 7:3, 1:1, and 3:7, *w/w*) under various a_w (dry to 0.44 a_w) and 30°C (*a* to *d*). The relationship between *S* and corresponding water content for studied solid matrices were fitted by Eq. (5) on the basis of k_{sp} (solid line) and k_{GT} (dash line) shown in *e* to *h*. The *S*

value of water involved in studied solid matrices (S_1) was extrapolated and compared to the literature data of liquid pure water (S_2) to interpret the water usability (Wu *et al.*, 2021).

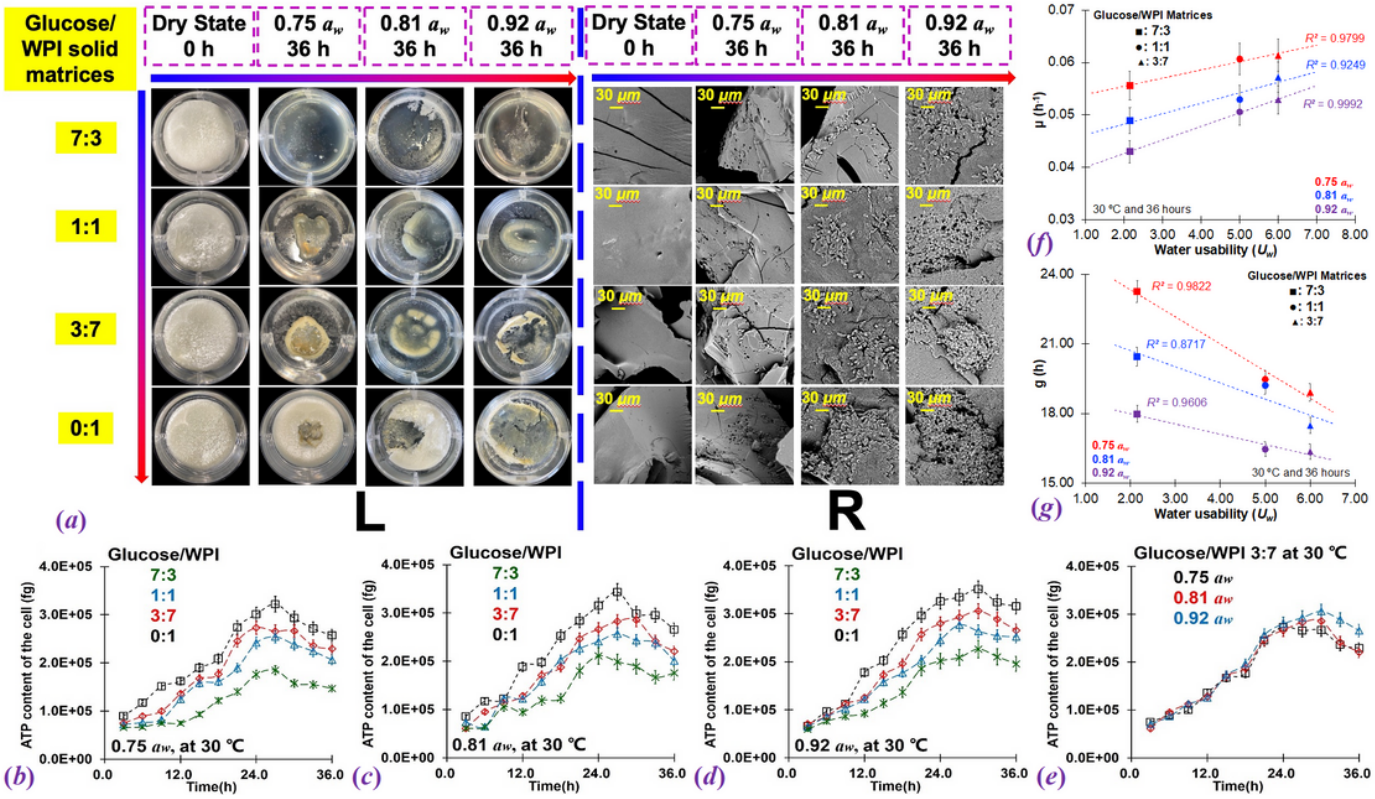

Figure 4

Photos (Left) and *SEM* images (Right) for the growth of *D. hansenii* in glucose/WPI solid matrices (7:3, 1:1, 3:7, and 0:1, w/w) after 36 hours of incubation at 0.75 to 0.92 a_w and 30 ºC (*a*). The corresponding growth curves of *D. hansenii* were shown from (*b*) to (*e*), and the relationship between the U_w and specific growth rate (μ) and cell doubling time (*g*) of *D. hansenii* were shown in (*f* and *g*).

Supplementary Files

This is a list of supplementary files associated with this preprint. Click to download.

- Supplementarymaterial.docx